Water Research 222 (2022) 118835

Contents lists available at ScienceDirect

Water Research

journal homepage: www.elsevier.com/locate/watres

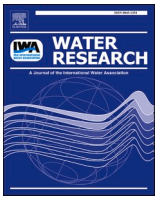

Quantification of 3-dimensional structure and properties of flocculated natural suspended sediment

K.L. Spencer [a,*], J.A. Wheatland [a,b], S.J. Carr [a,c], A.J. Manning [d], A.J. Bushby [a], C. Gu [a], L. Botto [a,e], T. Lawrence [a]

[a] School of Geography, Queen Mary University of London, Mile End Road, London E1 4NS, UK
[b] River Restoration Centre, St Albans, UK
[c] Institute of Science and Environment, University of Cumbria, Ambleside, Cumbria LA22 9BB, UK
[d] HR Wallingford, Howbery Park, Wallingford, Oxfordshire OX10 8BA, UK
[e] Department of Process and Energy, Delft University of Technology, Delft 2628 CB, the Netherlands

ARTICLE INFO

Keywords:
Density
Porosity, fractal dimension
Cohesive
Shape

ABSTRACT

Natural sediment flocs are fragile and highly heterogeneous aggregates of biogenic and minerogenic material typically with high porosity and low density. In aquatic environments dominated by fine, cohesive or mixed sediments they can dominate suspended sediment flux. Consequently, monitoring and modelling the behaviour, transport and distribution of flocs is very important for many aquatic industries, maintenance of waterways and conservation and management of aquatic waterbodies. Mathematical models that predict the behaviour of flocs rely on the accurate assessments of the size, shape, density, porosity and fractal dimension of flocs. These inherently 3-dimensional (3D) characteristics are typically derived from 2-dimensional (2D) data, largely due to the challenges associated with sampling, capturing, imaging and quantifying these fragile aggregates. We have developed new volumetric microscopy techniques which can quantify 3D internal and external structures and characteristics of sediment flocs. Here, these techniques were applied to quantify the 3D size (volume), shape and fractal dimension of natural and artificial sediment flocs and compare them to standard 2D approaches. Our study demonstrates that 2D approaches are under-estimating shape complexity and over-estimating the size and mass settling flux of flocs by up to two orders of magnitude, and the discrepancy between 2D and 3D is most marked for natural, organic rich macroflocs. Our study has significant implications for estimations of sediment flux at local to global scales within in aquatic environments. These new data and approaches offer the potential to improve the current parameterisation of sediment transport models and to improve the accuracy of current field-monitoring techniques.

1. Introduction

Natural sediment flocs are fragile, highly heterogeneous aggregates of minerogenic and biogenic material with fluid-filled pore space (Burd and Jackson, 2009; Droppo, 2001) and can represent the main component of suspended particulate matter (SPM) in both natural and engineered aquatic systems where sediment supply is dominated by fine-grained cohesive and mixed sediments (Mehta, 2013; Whitehouse et al., 2000). SPM transport is critical to the fate and flux of sediment (Manning and Dyer, 2007; Prandle et al., 2005; Spearman et al., 2020), carbon, nutrients, contaminants (Ye et al., 2021) and pathogens through all aquatic environments. Therefore, characterising flocs and predicting their dynamic behaviour is essential for the sustainable management of waterways, ports and harbours, fisheries and marine industries (Spearman et al., 2020; Winterwerp et al., 2006).

Floc behaviour is dependant upon the size, shape, fractal dimension, density and porosity of floc aggregates, and such data are critical input parameters for the mathematical models that predict fine sediment transport and flocculation (Dukhovskoy et al., 2021; Mehta et al., 2014; Sheremet et al., 2017). These characteristics are challenging to measure because flocs are fragile and difficult to sample without altering their structure (Many et al., 2019), and range in size from colloidal particles (nanometres) to larger aggregates (1000s microns) spanning multiple measurement and observation techniques. These characteristics are

* Corresponding author.
E-mail address: k.spencer@qmul.ac.uk (K.L. Spencer).

https://doi.org/10.1016/j.watres.2022.118835
Received 27 January 2022; Received in revised form 5 July 2022; Accepted 6 July 2022
Available online 7 July 2022

nearly always measured in 2 dimensions (2D): floc size, considered to be the most important parameter to determine settling velocity and is determined as the spherical or elliptical diameter of a 2D projection from video, image or laser analysis (Winterwerp, 1998); floc shape is commonly measured as simple 2D height to width ratios or shape parameters based on regression analysis, whilst some sediment transport models use characteristic shapes based on fractal mathematics (Lee et al., 2011; Moruzzi et al., 2020; Williams et al., 2008; Winterwerp, 1998); and fractal dimension, a proxy for floc complexity, is also usually derived in 2D (Smoczyński et al., 2016), with a fractal dimension of 1 indicating near spherical flocs, with larger values (up to 3) indicative of 'looser', more complex flocs. In addition, porosity and density which can influence settling behaviour through buoyancy and drag (as fluid flows through the floc) (Moruzzi et al., 2020) can only be estimated indirectly from settling velocity and assuming spherical shape. Therefore, these inherently 3-dimensional (3D) characteristics are only ever measured or estimated from 2D simplifications (Spencer et al., 2021).

Recently, new volumetric microscopy techniques have been developed and validated which can image and quantify 3D internal and external structures, characteristics and composition of sediment flocs with minimal disturbance (Spencer et al., 2021; Wheatland et al., 2020; Zhang et al., 2018). These operate across nano- to micro- scales and therefore, have the potential to quantify all meaningful floc characteristics including size, shape, fractal dimension, porosity and density (Spencer et al., 2021). In addition, we have developed techniques to capture and stabilise natural sediment flocs, whilst preserving these delicate 3D structures (Wheatland et al., 2017). The overall aim of this study was to quantify for the first time the detailed 3D geometry and structures of sediment flocs using X-ray microtomography (microCT). Our objectives were to quantify the 3D size, shape and fractal dimension of artificial and natural sediment flocs and compare these new quantitative 3D data to measurements derived using 2D image analysis techniques in a settling column. We then considered the application of these new 3D data streams to improve the accuracy and current application of 2D data with respects to 3D measurements and to improve our understanding and prediction of floc behaviour in the aquatic environment.

2. Methodology

2.1. General methodological approach

In order to compare the geometric structure and physical characteristics of flocs in both 2D and 3D we modified the Laboratory Spectral Flocculation Characteristics settling column and floc camera system (LabSFLOC) (Fig. 1) (Manning et al., 2017; Manning and Dyer, 2002). Floc images were captured as floc populations settled past the camera system to obtain 2D data. An agarose-filled plankton chamber was fitted to the bottom of the LabSFLOC column to capture and immobilise settled

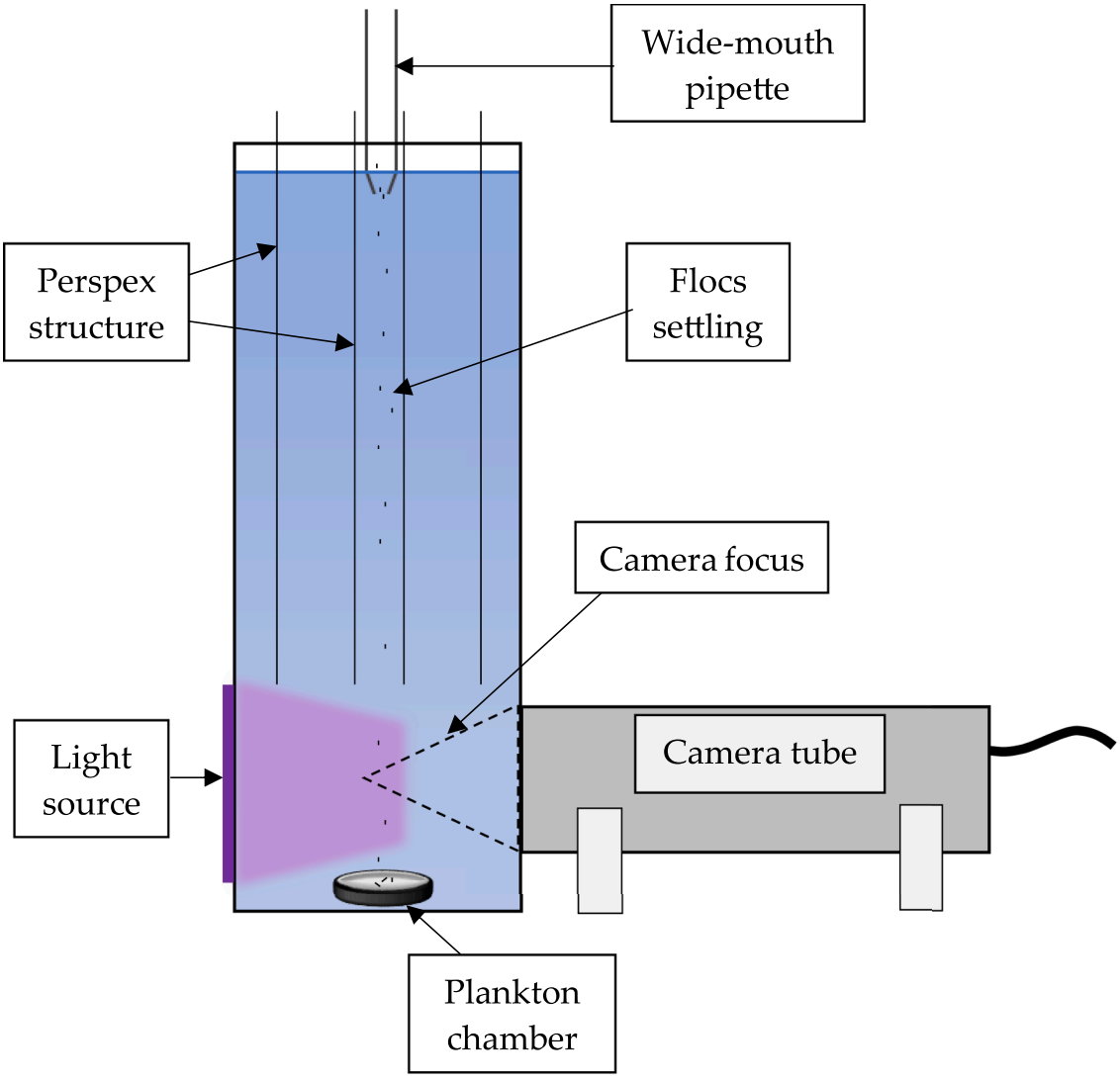

Fig. 1. Modified LabSFlOC settling column settling column and floc camera system.

flocs for analysis of 3D data by microCT. Thus, whilst it is not possible to match 2D and 3D measurements for individual flocs, we are sampling the same floc population in both 2D and 3D. Once the flocs had settled, the water within the LabSFLOC column was drained and the plankton chamber capped with a glass coverslip. The water within the plankton chamber was then exchanged with a saline solution (35 psu) containing low-melting-point electrophoresis-grade agarose at 0.75%. Plankton chambers were stored at 4 °C for 30 min to enable the agarose to solidify. These agarose discs contained 1000′s of individual flocs and were placed in sample holders and mounted on the microCT stage for scanning and analysis of 3D geometry. Flocs are very fragile and it is possible that sampling and processing may deform or modify their physical, chemical and biological characteristics. The agarose prevented any physical, chemical, or biological interactions between the flocs including minimising deformation during settling and sedimentation (Droppo et al., 1996), whilst the numbers of flocs collected were low enough not to overwhelm to the plankton chamber. Our methodological approach for capturing, stabilising and imaging fragile flocs in 3D is outlined in detail in Wheatland et al. (2017, 2020) and (Spencer et al., 2021) and successfully stabilised and preserved floc structures. Observations at the nanoscale 3D tomography demonstrated minimal shrinkage, deformation and/or alteration to 3D structure (Wheatland et al., 2017).

To optimise comparability between the 2D and 3D datasets, the resolution of microCT scans (voxel size 10 μm) was matched as closely as possible that of the LabSFLOC imagery (pixel size 6.7 μm).

Time requirements associated with data capture and computational processing mean that settling runs were not routinely replicated. However, in this study total sample number 'n' is very large (up to 10,000′s of flocs) and our focus was to compare the relative 2D and 3D characteristics of floc populations, rather than to quantify the characteristics of a floc population with given composition and physicochemical water column conditions.

2.2. Floc populations

Cohesive sediments were flocculated in a mini-annular flume in artificial seawater at 35 psu and a suspended particulate matter (SPM) concentration of 1.5 g L^{-1}. To examine wide ranging and contrasting floc sizes and shapes, four floc populations were considered; three 'artificial' flocs comprising bentonite clay and increasing concentrations of xanthan gum (proxy for organic matter) at 0.01%, 2% and 5% and a natural estuarine cohesive sediment sampled from the Thames Estuary, SE England, (silty clay, organic matter 15% based on loss on ignition). Flocs were extracted from the annular flume following 11-days suspension using a wide-mouthed pipette to avoid floc breakage (Manning and Dyer, 2002) and transferred to the modified LabSFLOC settling column.

2.3. Acquisition of 2D datasets

2D floc characteristic datasets including size (projected area and diameter) and shape (aspect ratio, circularity) were collected by recording floc images in the LabSFLOC using a high definition camera (Manning and Dyer, 2002; Ye et al., 2020) and processed using Trainable Weka (Arganda-Carreras et al., 2017) and Trackmate (Tinevez et al., 2017) packages within ImageJ.

2.4. Acquisition of 3D datasets

A detailed description of the use of microCT to acquire and quantify 3D volumetric floc datasets is provided in Wheatland et al. (2020). MicroCT scans were performed using a Nikon Metrology XT-H 225 (Tokyo, Japan) micro-tomograph. This scanner was configured with a 25–225 kV 0–2000 μA X-ray source with tungsten reflection target capable of generating polychromatic X-rays (focal spot size, c. 3 μm), and a Perkin Elmer (Waltham. Massachusetts, USA) 16-bit flat-panel detector. Scan parameters were set to optimise contrast and resolution (voltage 150 kV; current 160 μA; acquisition time between projections 2829 ms) with 2-frame averaging. Maintaining the same scan parameters for all X-ray datasets ensured that their greyscale values, and hence feature identification, would be comparable. The greyscale values of the resulting raw projections represented differences in X-ray energy attenuation, related to material density and the attenuation coefficient of the materials being imaged.

The X-ray microCT generated 2D projections of the sample that were reconstructed to generate 3D cubic data volumes for visualisation and quantification. The reconstruction of X-ray microCT datasets was conducted using CTPro 3D (Nikon, Tokyo, Japan). Each scan generated 1609 raw X-ray projections, yielding reconstructed volumes with dimensions of 2048 × 2048 × 2048 voxels with a voxel size of 10 μm. During reconstruction imaging artefacts (e.g., beam hardening, caused by the differential attenuation of X-rays through materials of differing density and thickness) (Ketcham and Carlson, 2001) were addressed by the application of specific algorithms.

2.5. Segmentation and quantification of 2D and 3D data

The quantification of both 2D and 3D data required material segmentation, i.e. the classification of material phases based on greyscale values and/or shape (Cnudde and Boone, 2013). Segmentation of the datasets generated binary images of each component (bulk phase), which was achieved in FIJI/ImageJ via using the semi-automated segmentation tool Trainable WEKA Segmentation (TWS) v2.1.0 capable of machine learning (Arganda-Carreras et al., 2017). Resulting binary volumes of each bulk phase were then quantified using the 2D Particle analyzer and 3D ROI Manager plugins (Ollion et al., 2013) in FIJI/ImageJ, which provided quantitative measurements of material properties, e.g., size, shape and greyscale intensities.

In the literature, flocs are frequently considered to be spherical objects due to the challenges of measuring their complex shapes and the ease of estimating their settling velocity by applying Stokes' Law (Khelifa and Hill, 2006; Many et al., 2019; Moruzzi et al., 2020). Our approach allows the quantification of the size of a complex 3D object (floc volume) and this was compared to standard approaches to assess floc size using equivalent spherical diameter (ESD); the perimeter diameter (D_{Perim}), surface equivalent diameter (D_{Surf}), circumscribing diameter (D_{Circum}) and the Feret diameter (D_{Feret}). Definitions are provided in Supporting Information, Table S1.

Shape was described using aspect ratio e.g., height to width ratios (2D and 3D), circularity (2D) and sphericity (3D). To measure the fractal dimension of the flocs from the voxel/pixel images, we used the sphere/circle packing method. Similar to the box-counting method, here circles were used to cover the area of the floc in 2D and spheres were used to cover the volume of the floc in 3D.

3. Results

Data from artificial and natural sediment flocs were combined to provide a dataset with wide-ranging floc characteristics and to compare relative 2D and 3D geometry. The number of flocs captured, observed and quantified varied considerably. In total, our dataset comprised observations for 22,744 flocs in 2D, i.e., images captured as they passed through the field of view for the LabSFLOC camera. However, as a large number of these flocs settled outside the plankton chamber and were not captured for analysis by microCT, a smaller population sub-set of 7974 flocs was quantified in 3D.

3.1. 2-Dimensional floc data

The particle size distribution measured as floc area is given in Fig. 2a and ranged from 40 μm^2 to $> 6 \times 10^5$ μm^2. This is a direct measurement of floc size based on occupied pixels, converted to a geometric scale

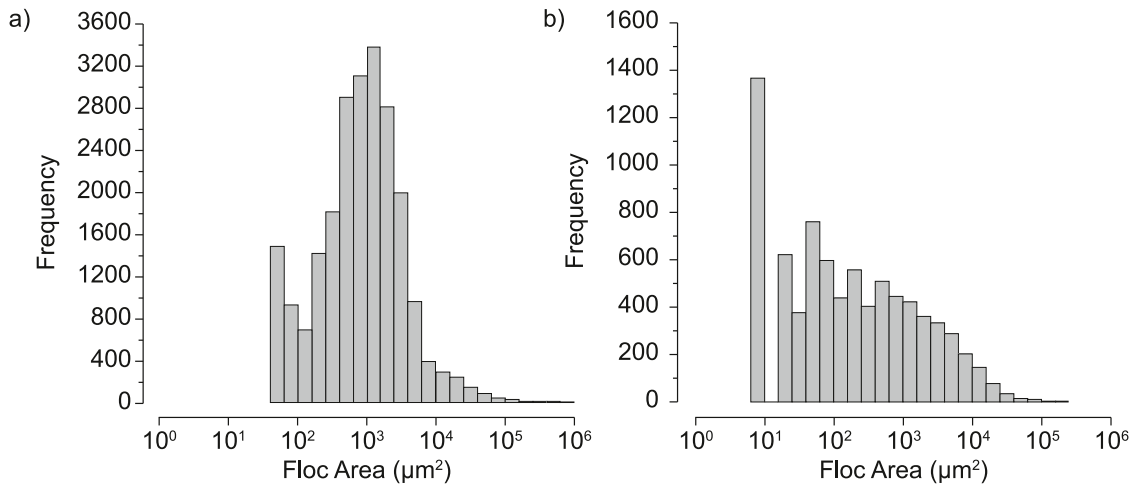

Fig. 2. Floc size distribution for a) 2D floc area (μm^2) and b) 3D floc volume (μm^3).

(micron) and shows a broadly bi-modal distribution with two population peaks and a median floc area of 889 μm^2.

To comply with conventions for measuring floc size and enable comparison between 2D and 3D data we created floc size distributions using equivalent spherical diameter (ESD); the perimeter diameter (D_{Perim}), surface equivalent diameter (D_{Surf}), circumscribing diameter (D_{Circum}) and the Feret diameter (D_{Feret}) (Fig. 3). All approaches show a broadly bi-modal floc size distribution. This aligns to previous *in situ* and laboratory observations of flocs indicating the presence of < c. 10 μm diameter flocs comprising flocculi and/or primary particles (Fettweis

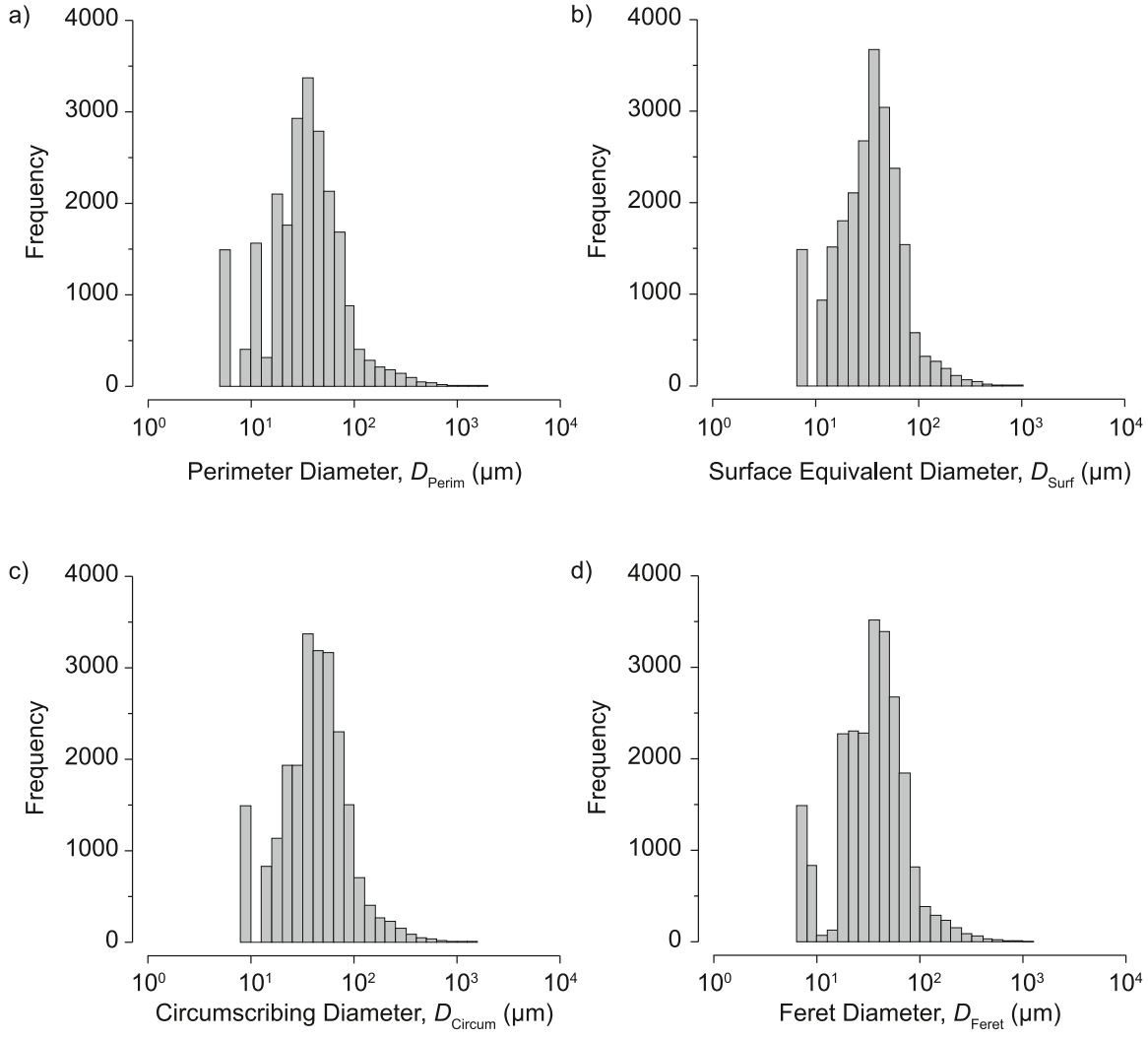

Fig. 3. Floc size distribution calculated from the 2D LabSFLOC data based on (a) the D_{Perim}, (b) the D_{Surf}, (c) the D_{Circum} and (d) the D_{Feret}.

et al., 2012; Shen et al., 2018; Spencer et al., 2021) and a larger floc population between c. 10 μm and >1000 μm diameter. This also appears a good representation of our samples comprising small, compact, low OM bentonite flocs through to large, organic rich, natural estuarine sediment flocs. The modal size of the smaller secondary population may not be observed due to our analytical detection limits and data filtering, and therefore the number of smaller flocs with diameter < 10 μm are almost certainly under-represented. Some authors observe further separations of these larger (> 10 μm) floc populations e.g., Manning and Schoellhamer (2013) observed separate floc populations with diameters < 160 μm (microflocs) and > 160 μm (macroflocs) but such distributions were not seen here and may indicate the dominance of smaller, artificial flocs in our population. The ESD was in the same order of magnitude for all approaches used, although d_{50} was greatest for D_{Circum}>D_{Feret}> D_{Perim}>D_{Surf} (ANOVA F(3, 90,972)=278, $p = 2.2 \times 10^{-16}$) and ranged from 34 – 43 μm, while d_{max} showed much greater variation ranging from 941–1814 μm (D_{Perim}>D_{Circum}>D_{Feret}>D_{Surf}).

Shape is also frequently used to characterise floc populations as it may be indicative of floc composition, with organic rich flocs having elongate 'stringer' shapes, and shape influences settling velocity and drag (Moruzzi et al., 2020). Individual flocs exhibited aspect ratios ranging from 1.0 to 9.1 (median 1.3) and circularity ranging from 0.09 to 1 (median = 1). Both measures indicate that the floc population is very strongly dominated by near-spherical flocs, again confirming the presence of small, compact flocs predominantly from our artificial floc populations. The majority of flocs had a fractal dimension between 1.5 and 2 in 2D, ranging from 1.02 to 2.25 with a median of 1.76 indicative of our compact simple artificial flocs and 'stringer' type natural sediment flocs.

3.2. 2-Dimensional floc data – 'macroflocs'

Larger flocs (here defined as those with D > 160 μm, e.g., Manning and Schoelhammer 2013) have been analysed separately from the total floc population as they tend to have more complex shapes and contribute significantly to mass settling flux (Manning and Dyer, 2007; Soulsby et al., 2013). The choice of approach for estimating ESD results in varying proportions of macroflocs (Table 1). Macroflocs contribute between 1.9% (D_{Surf}) to 3.6% (D_{Circum}) of the total population but between 40 and 50% of the total area occupied by the floc population (i.e., viewed and measured as projected areas in 2D). As expected, macroflocs have less spherical shapes with median H/L (c. 1.6) and median circularity (c. 0.5) showing little variation between the ESD characterisation methods used. Observations indicate that macroflocs are notably more variable in shape, and more elongate, indicative of larger, probably more organic rich flocs in our natural floc population.

3.3. 3-Dimensional floc data

The use of volumetric tomography enables quantification of floc size measured as occupied volume, and the floc volume distribution is shown in Fig. 2b. This again shows a broadly bimodal distribution, but now the smallest floc population (volume < 1000 μm^3) is much more dominant, although it may still be under-represented due to detection limitations.

Table 1
The number, percentage and area occupied by macroflocs (> 160 μm) depending on the diameter characterisation method used.

Diameter Characterisation Method	No. of Macroflocs	% of Total Population	Area Occupied by Macroflocs (μm^2)	% of Total Occupied Area
D_{Perim}	719	3.2	2.8×10^7	47.8
D_{Surf}	422	1.9	2.4×10^7	40.3
D_{Circum}	827	3.6	2.9×10^7	49.6
D_{Feret}	541	2.4	2.6×10^7	43.8

Floc volumes ranged from 1000 μm^3 (i.e., one voxel) to 1.9×10^7 μm^3, with a median floc volume of 12,996 μm^3. ESD was derived using the same approaches as the 2D data to enable comparison (Fig. 4). Floc ESD is in the same order of magnitude for all approaches, but there were significant differences in floc size (ANOVA, F(4, 31,892) = 150.6, $p = 2 \times 10^{-16}$) between the different calculation methods where d_{50} ranges between 29 and 37 μm (D_{Perim}>D_{Circum}>D_{Feret}>D_{Surf}) and D_{Max} ranged from 330 to 840 μm (D_{Circum}> D_{Feret}>D_{Perim}>D_{Surf}). The most striking difference is the relative dominance of the smaller floc population in the floc size distributions (Fig. 4a-d) and the bimodal distribution is far less pronounced when measured using D_{Feret}.

Adapting the approaches used in 2D, ESD was then used to estimate equivalent spherical volume (ESV) and compared to the measured floc volumes (occupied voxels) generated by microCT analysis (Table 2). There is a statistically significant over-estimation of volume when D_{Perim}, D_{Circum} and D_{Feret} are used [ANOVA F(4, 39,865)= 74.35, $p = 2 \times 10^{-16}$, followed by post hoc Tukey test] with the estimated median floc size doubled (D_{Perim}) and maximum floc size increased by up to an order of magnitude compared with the measured flocs.

Compared to measurements in 2D, 3D floc shape, measured as sphericity (3D equivalent of circularity), was less variable and far less spherical, ranging from 0.26 to 0.73 with a median value of 0.57, whilst aspect ratios varied from 1 to 3.5 indicative of much more elongate flocs. The majority of the flocs have a fractal dimension between 2.5 and 3 in 3D, with a median of 2.7 suggesting more complexity than the 2D measures.

3.4. 3-Dimensional floc data – 'macroflocs'

As for the 2D data, larger flocs > 160 μm diameter were analysed separately. The method for estimating ESD has far greater consequence on the estimation of macrofloc contribution to the floc population when derived from volume. For example, Table 3 demonstrates that macroflocs contribute between 1 and 5% of the total number of flocs, but between 27 and 66% of the total volume occupied by flocculated material. The shape of the macroflocs is again more complex and more elongate, with macrofloc sphericity ranging from 0.26 to 0.63, with most macroflocs having sphericity < 0.5.

4. Discussion

4.1. Floc size distribution

To enable statistical comparisons, both 2D and 3D data were filtered to account for differences in the limit of detection, hence particles $<3^2$ pixels (404 μm^2 LabSFLOC, 900 μm^2 micro CT) in 2D and $<3^3$ voxels (27,000 μm^3 micro CT) in 3D were excluded from the analysis. This means that for both populations the smallest flocs are not represented in the datasets, but the lower limit of detection across 2D and 3D data are broadly comparable.

Measuring floc size, as diameter, has been a key parameter in the assessment, monitoring and prediction of cohesive and mixed sediment behaviour as floc size is considered the most important control on settling velocity and hence fine and cohesive sediment dynamics (Williams et al., 2008). In this study we were able to directly quantify floc size from 2D projections and quantification of occupied pixels (area) as the floc population settled past the LabSFLOC camera, and in 3D as a measure of occupied volume. This is in contrast with most commonly-applied techniques in the field (e.g., Laser *In-Situ* Scattering and Transmissometry (LISST*), in situ* settling velocity instrument (INSSEV)) and laboratory (e.g., floc camera image analysis) that derive floc size data from 2D projections and use ellipse fitting to estimate ESD.

The most significant contrast between the two approaches is in the distribution of floc size. The distribution of floc area shows a clear bimodal distribution, and this is confirmed when observing the distribution of floc size using all four different measures of ESD. The bi-modal

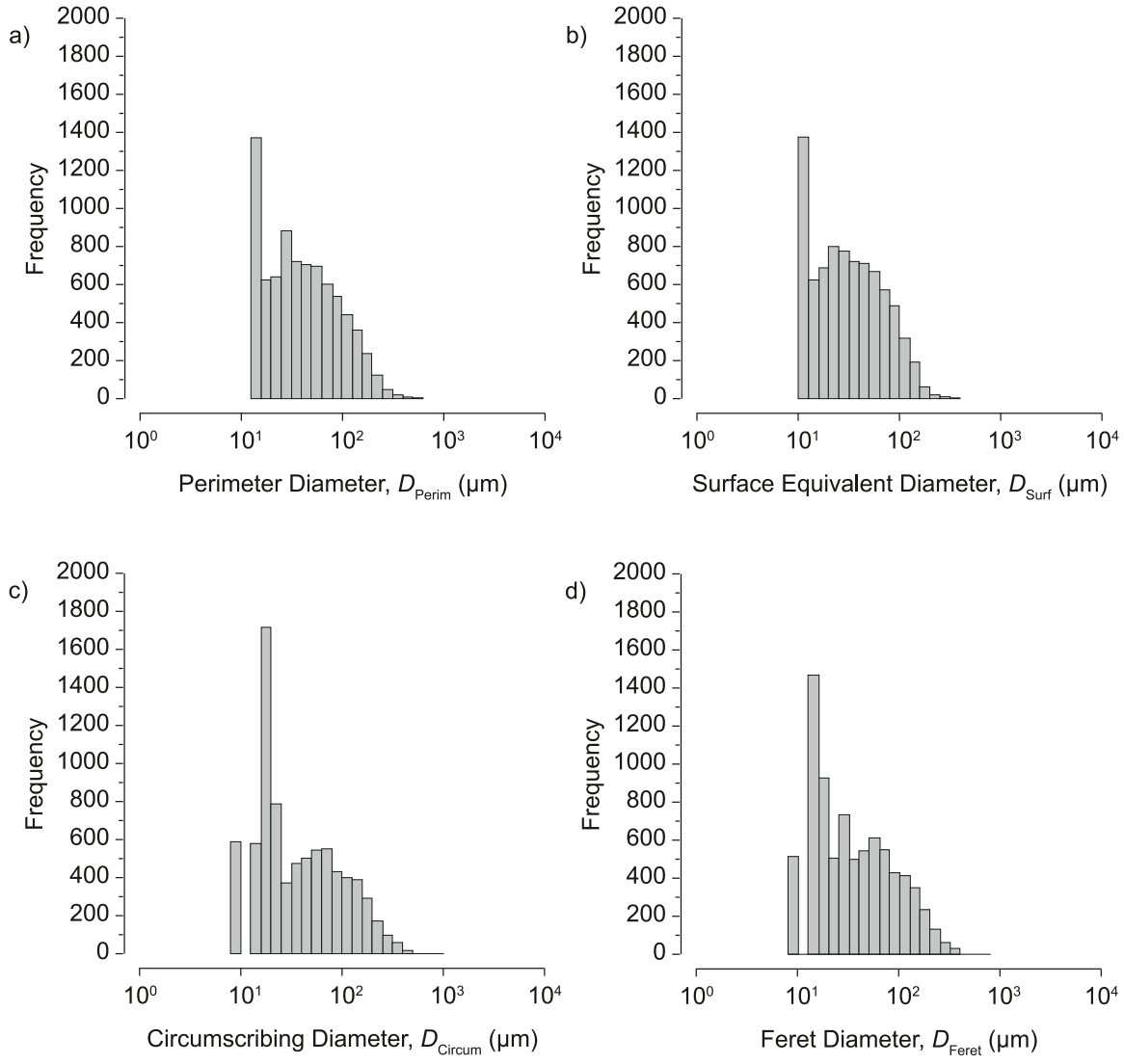

Fig. 4. Floc size distribution based on 3D data using equivalent floc diameter; (a) the D_{Feret}, (b) the D_{Surf}, (c) the D_{Circum} and (d) the D_{Perim}.

Table 2
Comparison of measured floc volume (microCT) and estimated equivalent spherical volume (ESV) based on four measures of equivalent spherical diameter and in μm^3.

Approach	Volume μm^3					
	Min.	1st Qu.	Median	Mean	3rd Qu.	Max.
(Measured) microCT (Estimated ESV)	1000	1999	1.3×10^4	1.6×10^5	8.8×10^4	1.9×10^7
Perimeter Diameter (D_{Perim})	1378	3908	2.6×10^4	4.8×10^5	2.0×10^5	1.3×10^8
Surface Equivalent Diameter (D_{Surf})	1000	1999	1.3×10^4	1.6×10^5	8.8×10^4	1.9×10^7
Circumscribing Diameter (D_{Circum})	522	2720	1.7×10^4	8.5×10^5	2.2×10^5	3.1×10^8
Feret Diameter (D_{Feret})	523	2490	1.5×10^4	5.5×10^5	1.7×10^5	2.4×10^8

distribution becomes most pronounced when using the Feret diameter as a measure of ESD, which is the most widely applied approach. The Feret diameter is a statistical measure of diameter, and is considered a valid estimate of floc size if sufficient measurements are made (as is the case here with > 20,000 floc measurements) as this accounts for any

Table 3
Differences in the number, percentage and area occupied by macroflocs depending on the diameter characterisation method used in the 3D dataset.

Diameter Characterisation Method	No. of Macroflocs	% of Total Population	Volume (μm^3) Occupied by Macroflocs	% of Total Occupied Volume
D_{Perim}	402	5.0	7.3×10^8	57.6
D_{Surf}	79	1.0	3.4×10^8	27.2
D_{Circum}	631	7.9	8.4×10^8	66.1
D_{Feret}	444	5.6	7.3×10^8	58.0

orientation of flocs as they settle (Jarvis et al., 2005). However, this bi-modal distribution becomes significantly less apparent when accurate measurements of floc size as volume are presented (Fig. 2b) and the distribution seen here is more of a size continuum, which is then dominated by the smallest class size of flocs (< 10 μm diameter). These observations are in contrast to the frequent reports of distinct multi-modal distributions of floc size derived from 2D data. These floc size distributions underpin 3D transport modelling of cohesive and mixed sediments by assigning variable fractal dimensions. Such observed multi-modal floc size distributions are caused by mixing of different sized particles and aggregates, particularly in coastal and estuarine settings (Lee et al., 2012) and are attributed to different

mechanisms of floc aggregation (Vahedi and Gorczyca, 2014) with two (e.g., (Mikkelsen et al., 2006), three (Shen et al., 2018) and four (Lee et al., 2012) levels of aggregation observed. Such levels of aggregation represent small, compact, highly spherical, primary particles and highly stable microflocs (or 'flocculi') which are dominated by electro-flocculation, and larger more complex floc aggregates where bio-flocculation and polymer bridging become increasingly important (Fettweis et al., 2012; Lee et al., 2012; Maggi, 2007). These multiple levels of floc aggregation (or floc 'hierarchy) are based on observations of multi-modal floc size distributions derived from 2D data and are used to assign variable fractal dimension and represent flocculation processes using multiple class population balance equations (PBE) (Shen et al., 2018). However, our 3D data, particularly for flocs > 10 μm diameter, demonstrate a continuum of floc size. This is supported by Spencer et al. (2021) who confirm that floc hierarchy is better defined by structure-function relationships rather than observations of geometric floc size distributions with key flocculation mechanisms operating across the floc size distribution. This suggests that multi-modal floc size distributions observed in 2D may be largely an artefact of how 2D size is measured rather than an accurate reflection of floc size modes with potential implications for the efficacy of predictive cohesive sediment transport models that use assigned variable fractal dimensions.

4.2. Quantifying floc size and shape

Floc size is generally reported assuming spherical/elliptical shape, either as equivalent spherical diameter (ESD) or e.g., the Sauter mean diameter (an equivalent volume/surface area ratio) used in *in situ* measurements using LISST sensors (Filippa et al., 2011). It is recognised that these are 2D measurements and may not capture the true floc morphology. Here, it is clear that floc size derived from 2D data, whether as counts of projected 2D area, or using multiple methods for the estimation of ESD, is over-estimated with respect to measurement of floc size (volume) quantified in 3D. These differences are modest and statistical measures to explore the population (e.g., median) are within the same order of magnitude. However, these differences become very significant when considering the largest flocs (D_{max}) and these over-estimations are most pronounced when using measures such as the perimeter or circumference equivalent spherical diameter which take into account the projected floc outline and are hence influenced by floc shape and complexity. This suggests that these over-estimations are likely due to the significant simplification of floc shape and become more pronounced when considering the larger 'macrofloc' populations (> 160 μm diameter) which contain our natural organic-rich flocculated estuarine sediments. The measures for floc shape are simplistic and we are restricted to aspect ratio (the ratio of smallest to longest diameter) which considers how elongate the floc is, and circularity/sphericity (relationship between the floc perimeter and area/volume) which roughly describes how irregular the shapes are relative to a simple circle or sphere. 3D measurements indicate that flocs are far more elongate and irregular in shape compared to 2D measurements. Recent 3D imagery of natural estuarine sediment flocs confirms the complexity and shape irregularity of natural sediment flocs and the influence of biological populations on floc shape (Spencer et al., 2021; Wheatland et al., 2020, 2017). Therefore, measures of floc size in controlled laboratory experiments using simple minerogenic sediments are likely to provide good estimations of floc size, but this becomes increasingly unreliable for natural, organic rich sediments.

The over-estimation of floc size in 2D has been previously recognised, particularly where flocs become preferentially orientated during settling presenting the longest axis to the floc camera (Jarvis et al., 2005). However, the over-simplification of floc shape in 2D may have additional consequences. Firstly, over-estimation of size is more significant for the largest flocs which have more complex and elongate shapes and this may result in the artificial creation of a bimodal floc distribution, where larger flocs become over-represented in the floc population. This is confirmed by a more continuous size distribution when size is quantified from 3D data. Secondly, estimations of floc size from 2D projections and estimates of ESD will result in a significant amount of empty space surrounding the floc being attributed to the floc with significant consequences for the estimations of floc density and porosity which are typically derived from settling velocity and assumptions of spherical shape utilising Stokes' Law.

4.3. Consequences for understanding and predicting the dynamics of cohesive and mixed sediments

Floc size (diameter) is considered to be the most important floc parameter influencing settling velocity (Droppo, 2001; Fennessy et al., 1994; Gibbs, 1985; Li and Ganczarczyk, 1987). However, shape, porosity and density also have an impact with shape affecting drag, density having an influence on the force driving settling velocity and porosity through affecting internal friction as water moves through the floc body (Li and Ganczarczyk, 1988; Wu and Lee, 1998). These 3D data suggest that we are currently under-estimating or inadequately representing floc shape and/or irregularity. This results in over-estimation of floc size by up to an order of magnitude for large, organic-rich, natural sediment flocs and means that we are probably over-estimating floc porosity by including empty space surrounding irregular shaped flocs and thus by default underestimating floc density. The frequently-observed relationships between increasing floc size and decreasing density/increasing porosity (Fennessy et al., 1994; Gibbs, 1985) have dictated the application of fractal mathematics to account for floc variability in cohesive sediment transport modelling. Yet, these data suggest that our estimations of density and porosity are better explained by increasing floc complexity and shape irregularity with size, particularly for natural sediments and this may confirm some observations of the relationships between floc density and shape (Choi et al., 2018). In addition, there is increasing evidence that floc shape (both variability and complexity) has a significant impact on settling velocity, although floc shape is rarely measured (Choi et al., 2018; Many et al., 2019). These new data now provide the opportunity to develop algorithms that significantly improve the characterisation and quantification of floc shape parameters, as well as direct quantification of floc size and porosity.

Over-estimating floc size may have significant consequences for estimation of the flux of sediment, carbon, nutrients and pollutants through the aquatic environment. To explore the potential impact on mass settling flux we used average floc effective density values for microfloc (D<160 μm, 200 kg m^{-3}) and macrofloc (D>160 μm, 50 kg m^{-3}) fractions from 207 data sets (i.e. individual floc populations) from the Tamar (UK), Gironde (France), and Dollard (Netherlands) estuaries (Manning and Dyer, 2007) (suspended sediment concentrations between 5 mg L^{-1} and 8600 mg L^{-1}). Then using both floc volume quantified in 3D, and estimated from the 2D Feret ESD, we estimated floc mass. Considering median floc size there is no significant difference in the data, suggesting that for the majority of our simple, compact, near spherical artificial flocs that the use of 2D data makes little difference to estimations of mass settling flux. This is expected, as near-spherical flocs are approximately rotationally symmetric, thus a 2D projection contains comparable information to the full 3D geometry. However, for the largest flocs the use of 2D data over-estimates floc mass by up to 1 order of magnitude for the microfloc populations and two orders of magnitude for the macrofloc populations. Whilst these calculations are approximations, they are indicative of the substantial errors that may be propagated by modelling approaches that rely on 2D floc size, particularly where natural sediments are forming large, EPS-rich, organic flocs with complex and/or elongate shapes.

The imaging and data-processing approaches used here are operator- and computer processor-intensive. Therefore, at present our approach is unlikely to be adapted for application as part of e.g., a field monitoring campaign without significant modification. However, the coupled 2D/

3D methodological approach allows accurate quantification of the errors associated with 2D measurements and enables geometric measures of 3D floc structure (size, shape, porosity, density) to be related to measures of floc dynamics such as settling velocity and flocculation rates. The possibility of translating 2D data to 3D predictions via simple relations was explored, and a power-law relation with an exponent slightly larger than 2 was found ($y = 0.702*x^{2.394}$). Whilst it is not yet clear whether this result is universal for all flocs with varying composition, the use of a simple power-law relationship between 2D and 3D data provides an approach whereby current field-based techniques such as LISST can provide significantly more realistic measures of the complex structures and characteristics of natural, heterogeneous sediment flocs.

5. Conclusions

- X-ray microtomography offers the opportunity to quantify the 3D structure and physical properties of artificial and natural sediment flocs including volumetric size, floc size distribution and shape across a range of scales from a few to 1000s microns.
- New 3D data indicate that bi- and multi-modal floc size distributions which are typically used to assign variable fractal dimensions may be an artefact of 2D simplification of complex 3D shapes.
- New 3D data demonstrate a level of complexity and irregularity in floc shape characteristics that cannot be accounted for in 2D shape descriptors. This indicates that porosity may also be over-estimated for flocs.
- Measuring floc size assuming spherical or elliptical shapes from 2D projections over-estimates the size of individual flocs and the mass of flocculated material by up to two orders of magnitude. This is most pertinent for natural, large, highly organic flocs and has consequences for estimations of the flux of sediment, carbon and nutrients through aquatic environments.

Author contribution

KLS and AJB conceived the project. KLS wrote the manuscript with JATW. JATW collected and analysed the datasets. SJC, TL and AJB contributed to analysis of 3D datasets. AJM and LB contributed expertise to experimental design and interpretation of floc data. All authors contributed to interpretation, discussion and editing of the manuscript.

Declaration of Competing Interest

The authors declare the following financial interests/personal relationships which may be considered as potential competing interests: Kate Spencer, Jonathan Wheatland, Andrew Bushby, Simon Carr, Lorenzo Botto, Tom Lawrence reports financial support was provided by Natural Environment Research Council. Andrew Manning reports financial support was provided by US Natural Science Foundation.

Acknowledgments

This research was supported by the Natural Environment Research Council (grant number NE/011678/1 and NE/M009726/1). AJM's contribution towards this research was also partly supported by the US National Science Foundation under grants OCE-1736668 and OCE-1924532, TKI-MUSA Project 11204950–000-ZKS-0002, and HR Wallingford Company Research FineScale Project (ACK3013_62). The authors would like to thank Michelle Day for assistance with the 3D X-Ray microtomography. All laboratory work was conducted in the School of Geography, Queen Mary University of London.

Supplementary materials

Supplementary material associated with this article can be found, in the online version, at doi:10.1016/j.watres.2022.118835.

References

Arganda-Carreras, I., Kaynig, V., Rueden, C., Eliceiri, K.W., Schindelin, J., Cardona, A., Sebastian Seung, H., 2017. Trainable Weka Segmentation: a machine learning tool for microscopy pixel classification. Bioinformatics 33, 2424–2426. https://doi.org/10.1093/bioinformatics/btx180.

Burd, A.B., Jackson, G.A., 2009. Particle aggregation. Annu. Rev. Mar. Sci. 1, 65–90. https://doi.org/10.1146/annurev.marine.010908.163904.

Choi, S.M., Seo, J.Y., Ha, H.K., Lee, G., 2018. Estimating effective density of cohesive sediment using shape factors from holographic images. Estuar. Coast. Shelf Sci. 215, 144–151. https://doi.org/10.1016/j.ecss.2018.10.008.

Cnudde, V., Boone, M.N., 2013. High-resolution X-ray computed tomography in geosciences: a review of the current technology and applications. Earth Sci. Rev. 123, 1–17. https://doi.org/10.1016/j.earscirev.2013.04.003.

Droppo, I.G., 2001. Rethinking what constitutes suspended sediment. Hydrol. Process. 15, 1551–1564. https://doi.org/10.1002/hyp.228.

Droppo, I.G., Flannigan, D.T., Leppard, G.G., Jaskot, C., Liss, S.N., 1996. Floc stabilization for multiple microscopic techniques. Appl. Environ. Microbiol. 62, 3508–3515. https://doi.org/10.1128/AEM.62.9.3508-3515.1996.

Dukhovskoy, D.S., Morey, S.L., Chassignet, E.P., Chen, X., Coles, V.J., Cui, L., Harris, C. K., Hetland, R., Hsu, T.-J., Manning, A.J., Stukel, M., Thyng, K., Wang, J., 2021. Development of the CSOMIO coupled ocean-oil-sediment- biology model. Front. Mar. Sci. 8, 629299 https://doi.org/10.3389/fmars.2021.629299.

Fennessy, M.J., Dyer, K.R., Huntley, D.A., 1994. inssev: an instrument to measure the size and settling velocity of flocs *in situ*. Mar. Geol. 117, 107–117. https://doi.org/10.1016/0025-3227(94)90009-4.

Fettweis, M., Baeye, M., Lee, B.J., Chen, P., Yu, J.C.S., 2012. Hydro-meteorological influences and multimodal suspended particle size distributions in the Belgian nearshore area (southern North Sea). Geo-Mar. Lett. 32, 123–137. https://doi.org/10.1007/s00367-011-0266-7.

Filippa, L., Freire, L., Trento, A., Álvarez, A.M., Gallo, M., Vinzón, S., 2011. Laboratory evaluation of two LISST-25X using river sediments. Sediment. Geol. 238, 268–276. https://doi.org/10.1016/j.sedgeo.2011.04.017.

Gibbs, R.J., 1985. Settling velocity, diameter, and density for flocs of illite, kaolinite, and montmorillonite. SEPM J. Sediment. Res. Vol. 55 https://doi.org/10.1306/212F860C-2B24-11D7-8648000102C1865D.

Jarvis, P., Jefferson, B., Parsons, S.A., 2005. Measuring floc structural characteristics. Rev. Environ. Sci. Biotechnol. 4, 1–18. https://doi.org/10.1007/s11157-005-7092-1.

Ketcham, R.A., Carlson, W.D., 2001. Acquisition, optimization and interpretation of X-ray computed tomographic imagery: applications to the geosciences. Comput. Geosci. 27, 381–400. https://doi.org/10.1016/S0098-3004(00)00116-3.

Khelifa, A., Hill, P.S., 2006. Models for effective density and settling velocity of flocs. J. Hydraul. Res. 44, 390–401. https://doi.org/10.1080/00221686.2006.9521690.

Lee, B.J., Fettweis, M., Toorman, E., Molz, F.J., 2012. Multimodality of a particle size distribution of cohesive suspended particulate matters in a coastal zone: a multimodal PSD of cohesive sediments. J. Geophys. Res. Oceans 117. https://doi.org/10.1029/2011JC007552 n/a-n/a.

Lee, B.J., Toorman, E., Molz, F.J., Wang, J., 2011. A two-class population balance equation yielding bimodal flocculation of marine or estuarine sediments. Water Res. 45, 2131–2145. https://doi.org/10.1016/j.watres.2010.12.028.

Li, D., Ganczarczyk, J., 1988. Flow through activated sludge flocs. Water Res. 22, 789–792. https://doi.org/10.1016/0043-1354(88)90192-3.

Li, D.-H., Ganczarczyk, J.J., 1987. Stroboscopic determination of settling velocity, size and porosity of activated sludge flocs. Water Res. 21, 257–262. https://doi.org/10.1016/0043-1354(87)90203-X.

Maggi, F., 2007. Variable fractal dimension: a major control for floc structure and flocculation kinematics of suspended cohesive sediment. J. Geophys. Res. 112, C07012. https://doi.org/10.1029/2006JC003951.

Manning, A.J., Dyer, K.R., 2007. Mass settling flux of fine sediments in Northern European estuaries: measurements and predictions. Mar. Geol. 245, 107–122. https://doi.org/10.1016/j.margeo.2007.07.005.

Manning, A.J., Dyer, K.R., 2002. The use of optics for the *in situ* determination of flocculated mud characteristics. J. Opt. Pure Appl. Opt. 4, S71–S81. https://doi.org/10.1088/1464-4258/4/4/366.

Manning, A.J., Schoellhamer, D.H., 2013. Factors controlling floc settling velocity along a longitudinal estuarine transect. Mar. Geol. 345, 266–280. https://doi.org/10.1016/j.margeo.2013.06.018.

Manning, A.J., Whitehouse, R.J.S., Uncles, R.J., 2017. Suspended particulate matter: the measurement of Flocs. In: Uncles, R.J., Mitchell, S.B. (Eds.), Estuarine and Coastal Hydrography and Sediment Transport. Cambridge University Press, Cambridge, pp. 211–260. https://doi.org/10.1017/9781139644426.009.

Many, G., Durrieu de Madron, X., Verney, R., Bourrin, F., Renosh, P.R., Jourdin, F., Gangloff, A., 2019. Geometry, fractal dimension and settling velocity of flocs during flooding conditions in the Rhône ROFI. Estuar. Coast. Shelf Sci. 219, 1–13. https://doi.org/10.1016/j.ecss.2019.01.017.

Mehta, A.J., 2013. An Introduction to Hydraulics of Fine Sediment Transport. World Scientific. Advanced Series on Ocean Engineering.

Mehta, A.J., Manning, A.J., Khare, Y.P., 2014. A note on the Krone deposition equation and significance of floc aggregation. Mar. Geol. 354, 34–39. https://doi.org/10.1016/j.margeo.2014.04.002.

Mikkelsen, O.A., Hill, P.S., Milligan, T.G., 2006. Single-grain, microfloc and macrofloc volume variations observed with a LISST-100 and a digital floc camera. J. Sea Res. 55, 87–102. https://doi.org/10.1016/j.seares.2005.09.003.

Moruzzi, R.B., Bridgeman, J., Silva, P.A.G., 2020. A combined experimental and numerical approach to the assessment of floc settling velocity using fractal geometry. Water Sci. Technol. 81, 915–924. https://doi.org/10.2166/wst.2020.171.

Ollion, J., Cochennec, J., Loll, F., Escudé, C., Boudier, T., 2013. TANGO: a generic tool for high-throughput 3D image analysis for studying nuclear organization. Bioinformatics 29, 1840–1841. https://doi.org/10.1093/bioinformatics/btt276.

Prandle, D., Lane, A., Manning, A.J., 2005. Estuaries are not so unique. Geophys. Res. Lett. 32, L23614. https://doi.org/10.1029/2005GL024797.

Shen, X., Lee, B.J., Fettweis, M., Toorman, E.A., 2018. A tri-modal flocculation model coupled with TELEMAC for estuarine muds both in the laboratory and in the field. Water Res. 145, 473–486. https://doi.org/10.1016/j.watres.2018.08.062.

Sheremet, A., Sahin, C., Manning, A.J., 2017. Flocculation: a general aggregation-fragmentation framework. Coast. Eng. Proc. 27 https://doi.org/10.9753/icce.v35.sediment.27.

Smoczyński, L., Ratnaweera, H., Kosobucka, M., Smoczyński, M., Kalinowski, S., Kvaal, K., 2016. Modelling the structure of sludge aggregates. Environ. Technol. 37, 1122–1132. https://doi.org/10.1080/09593330.2015.1102332.

Soulsby, R.L., Manning, A.J., Spearman, J., Whitehouse, R.J.S., 2013. Settling velocity and mass settling flux of flocculated estuarine sediments. Mar. Geol. 339, 1–12. https://doi.org/10.1016/j.margeo.2013.04.006.

Spearman, J., Taylor, J., Crossouard, N., Cooper, A., Turnbull, M., Manning, A., Lee, M., Murton, B., 2020. Measurement and modelling of deep sea sediment plumes and implications for deep sea mining. Sci. Rep. 10, 5075. https://doi.org/10.1038/s41598-020-61837-y.

Spencer, K.L., Wheatland, J.A.T., Bushby, A.J., Carr, S.J., Droppo, I.G., Manning, A.J., 2021. A structure–function based approach to floc hierarchy and evidence for the non-fractal nature of natural sediment flocs. Sci. Rep. 11, 14012. https://doi.org/10.1038/s41598-021-93302-9.

Tinevez, J.-.Y., Perry, N., Schindelin, J., Hoopes, G.M., Reynolds, G.D., Laplantine, E., Bednarek, S.Y., Shorte, S.L., Eliceiri, K.W., 2017. TrackMate: an open and extensible platform for single-particle tracking. Methods 115, 80–90. https://doi.org/10.1016/j.ymeth.2016.09.016.

Vahedi, A., Gorczyca, B., 2014. Settling velocities of multifractal flocs formed in chemical coagulation process. Water Res. 53, 322–328. https://doi.org/10.1016/j.watres.2014.01.008.

Wheatland, J.A.T., Bushby, A.J., Spencer, K.L., 2017. Quantifying the structure and composition of flocculated suspended particulate matter using focused ion beam nanotomography. Environ. Sci. Technol. 51, 8917–8925. https://doi.org/10.1021/acs.est.7b00770.

Wheatland, J.A.T., Spencer, K.L., Droppo, I.G., Carr, S.J., Bushby, A.J., 2020. Development of novel 2D and 3D correlative microscopy to characterise the composition and multiscale structure of suspended sediment aggregates. Cont. Shelf Res. 200, 104112 https://doi.org/10.1016/j.csr.2020.104112.

Whitehouse, R., Soulsby, R., Roberts, W., Mitchener, H., 2000. Dynamics of Estuarine Muds. Thomas Telford Publishing. https://doi.org/10.1680/doem.28647.

Williams, N.D., Walling, D.E., Leeks, G.J.L., 2008. An analysis of the factors contributing to the settling potential of fine fluvial sediment. Hydrol. Process. 22, 4153–4162. https://doi.org/10.1002/hyp.7015.

Winterwerp, J.C., 1998. A simple model for turbulence induced flocculation of cohesive sediment. J. Hydraul. Res. 36, 309–326. https://doi.org/10.1080/00221689809498621.

Winterwerp, J.C., Manning, A.J., Martens, C., de Mulder, T., Vanlede, J., 2006. A heuristic formula for turbulence-induced flocculation of cohesive sediment. Estuar. Coast. Shelf Sci. 68, 195–207. https://doi.org/10.1016/j.ecss.2006.02.003.

Wu, R.M., Lee, D.J., 1998. Hydrodynamic drag force exerted on a moving floc and its implication to free-settling tests. Water Res. 32, 760–768. https://doi.org/10.1016/S0043-1354(97)00320-5.

Ye, L., Manning, A.J., Holyoke, J., Penaloza-Giraldo, J.A., Hsu, T.-.J., 2021. The role of biophysical stickiness on oil-mineral flocculation and settling in seawater. Front. Mar. Sci. 8, 628827 https://doi.org/10.3389/fmars.2021.628827.

Ye, L., Manning, A.J., Hsu, T.-.J., 2020. Oil-mineral flocculation and settling velocity in saline water. Water Res. 173, 115569 https://doi.org/10.1016/j.watres.2020.115569.

Zhang, N., Thompson, C.E.L., Townend, I.H., Rankin, K.E., Paterson, D.M., Manning, A.J., 2018. Nondestructive 3D Imaging and quantification of hydrated biofilm-sediment aggregates using x-ray microcomputed tomography. Environ. Sci. Technol. 52, 13306–13313. https://doi.org/10.1021/acs.est.8b03997.